Applied Mathematics & Information Sciences
An International Journal

Experimental Research on the Instability Characteristics of Double-layer Rock Plates Based on MTS-AE System

Shuren Wang[1,3], *Paul Hagan*[2] *and Yan Cheng*[2]

[1]School of Civil Engineering and Mechanics, Yanshan University, Qinhuangdao, 066004 P. R. China
[2]School of Mining Engineering, University of New South Wales, Sydney, 2052 Australia
[3]Key Laboratory of Mechanical Reliability for Heavy Equipments and Large Structures, Qinhuangdao, 066004 P. R. China

Received: 19 Jul. 2012, Revised: 19 Oct. 2012, Accepted: 30 Oct. 2012
Published online: 1 Feb. 2013

Abstract: The deformation and failure process of four classes of double-layer rock plates were researched experimentally with the new loading device under concentrated load based on MTS-AE system. The force-displacement curves and the force-time-acoustic emission event rate curves were obtained through the experiments. The results showed that there were three failure modes of beam fracture, arch destruction and plate fracture damage in the upper plate of the double-layer rock plates; all the lower plates of the four classes of rock plates produced the beam fracture damage. There were four distinct mechanical response stages in the force-displacement curves; three types of mechanical behavior of the double-layer rock plates arose after the second load peak, which were post-peak yielding, post-peak hardening and post-peak softening; the bearing capacity of the double-layer rock plates is usually greater than that of the single-layer rock plate. It showed that the acoustic emission events were not only in the phase before the peak value, but also in the post-peak phase.

Keywords: Rock plate, acoustic emission, laboratory test, mined-out areas.

1. Introduction

In the past three decades, numerous shallow mined-out areas had been left due to disordered mining by private coal mines in China. With the decrease of available land resources, a number of industrial and civil buildings, and many structures such as expressways, bridges and tunnels had to cross the mined-out areas. The stress of overlying strata in shallow mined-out areas was redistributed after the coal being mined, and then ground subsidence and destruction of these buildings appeared, which seriously affected the building plan, construction and operation of the structures built above the mined-out areas [1].

The layered sedimentary strata structure was the common structure type of the rock roof in the coal mined-out areas. Considering the effect of the bedding structure, the characteristics of transverse isotropy and the interaction between layers, the deformation feature, failure mode and fracture mechanism of the layered roof were more complicated. Thus, it is the difficult problem that needs to be urgently solved to study on the roof deformation and failure process and catastrophe mechanism in engineering practice.

At present, on one hand, most scholars at home and abroad usually regarded the roof of mined-out areas as the rock beam to do mechanical analysis and the relevant tests [2-6]. The processing method simplified the analytic process but it has apparent limitations, which can not reflect the spatial effect and the anisotropic of the roof, so the reliability of the results caused unavoidably doubt. On the other hand, most analysis and design are based on the thin plate theory, while the practical ratio of length to thickness of the roof could not meet the requirement of the thin plate theory [7-9]. In practical mining engineering, the major deformation and failure of the roof of the mined-out areas mostly performed rock-plate types, further more it usually expressed the layered rock plates. Therefore, it is necessary to develop and design a new loading device which could simulate the process of the deformation of thin plates, thick plates or thin-thick combined plates, which is the key to study on the deformation and failure process and catastrophe mechanism of the roof of the mined-out areas [10-15].

* Corresponding author e-mail: w_sr88@163.com

2. Experimental Design

2.1. Sandstone samples and test programs

The rock samples used in the test were Hawkesbury sandstone, which obtained from Gosford Quarry in Sydney, Australia. The quartz sandstones which contained a small quantity of feldspars, siderite, and clay minerals were formed in marine sedimentary basin of the mid-Triassic, and located on the top of coal-bearing strata. The surface of specimen exhibited local red rather than usual white because of the content and distribution of iron oxide.

For the single-layer roof of the mined-out areas, it could be classified into two categories according to the thickness: the thin plate and the thick plate. And the roof was always made up of various combinations of the thin plates and the thick plates. Thus, according to the definition of the thin plate and the thick plate in elastic mechanics, the specimen size of the thick plate was deigned to 190 mm ×75 mm × 24 mm (length, width, and thickness) and that of the thin plate was deigned to 190 mm × 75 mm × 14 mm (length, width, and thickness). According to the sizes above mentioned, the specimens was obtained by cutting the same sandstone in the laboratory of School of Mining Engineering, University of New South Wales. The physical-mechanical parameters of rock plates were shown in Table 1.

Under the concentrated load, the double-layer rock plates contacted closely, and performed the bending deformation together; the frictional resistance caused by slide between these two plates could reflect the mechanical effects of the interaction to some extent.

In the test, these double-layer rock plates were classified into four categories: upper thin plate and lower thick plate, upper thick plate and lower thin plate, double-layer thin plates and double-layer thick plates. Every sort of rock plates were produced for three sets and the comparative tests were done under the same conditions.

Table 1 Physical-mechanical parameters of rock plates.

Name	D (kg·m^{-3})	E (GPa)	v	C (MPa)	F (^{o})	T (MPa)	Cs (MPa)
Sandstone	2650	2.7	0.2	2.8	45	0.95	13.5
Notes	D-Density; E-Elastic modulus; v-Poisson ratio; C-Cohesion; F-Friction angle; T-Tensile strength; C*s*-Compression strength.						

2.2. Loading devices and loading modes

As shown in Fig. 1, the new loading device for rock plates bending test had already been authorized the utility model patent by State Intellectual Property Office of the P.R.C. (ZL201120284625.7).

The device consisted of three parts: the top was the circular board used to load concentratedly, the middle was loading framework which included four bolts with nuts connecting the steel plates on both sides, and the bottom was rectangle steel foundation, the rotatable hinge supports were set to connect the steel plates on both sides of the loading framework (Fig. 1).

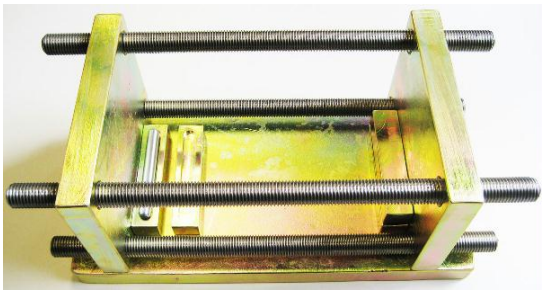

Figure 1 Loading device schematic for rock plates test.

Since the overlying rock above the layered roof was usually treated as the uniform load, it is the key problem for how to apply the uniform load continuously on the layered roof in the process of the test. To simplify the stress condition reasonably, the uniform load was identified with the concentrated load through analyzing again and again. So the loading circular plate which steel ball was embedded in (Fig. 2) was selected to match the contactor of MTS test machine.

Figure 2 Loading circular plate.

2.3. Ends design and connection method

Whether the design of double-layer rock plate's ends was reasonable or not were the key point to the test.

In the test, the boundary restraint state of these two ends was reasonably simulated to avoid that the stiffness was too high or too small, which played the decisive role to reveal the deformation process and fracture mechanism.

Generally, the constraint forms of rock plate's ends was classified into three categories: hinged-support boundary, fixed supported boundary and unconstrained boundary. To simulate the real boundary restraint of the roof of the mined-out areas, this test selected the first boundary constraint form that the displacement along the width of the rock plate was restricted, and the ends along the length of the rock plate were simply supported. And some special designs were used as followed: the curved groove along the length of the hinge bearing was designed to place a cylindrical ball. When the special designs were used, the movable bearing should be put on the fixed base in which the cylindrical steel was built to cause the free bending of the rock plate's end along one direction in order to achieve the restraint of the hinge bearing (Fig. 3).

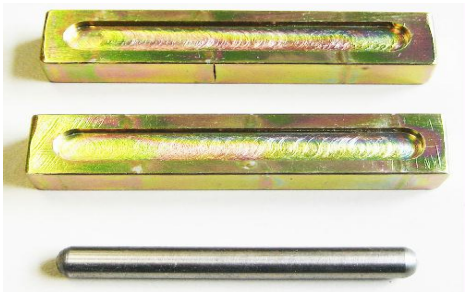

Figure 3 Hinge bearing design.

2.4. Test loading and data acquisition system

The loading device selected was MTS-851 rock mechanics testing machine, and the load was controlled by axial displacement and the loading rate was 110-2 mm/s (Fig. 4). The measure of axial load value and axial displacement value could be performed in real time by data acquisition system automatically.

The bridge modules of acoustic emission (AE) data acquisition were from American National Instruments and these models were Ni 9237, Ni 9205 and Ni 9201, which were based on Labview software platform and AE signals could be analyzed (Fig. 5). In the test, the sampling frequency of AE monitoring data was set to 50 kS/s, and the cumulative value of acoustic emission event could be read at regular intervals.

Figure 4 MTS-851 rock mechanics testing machine.

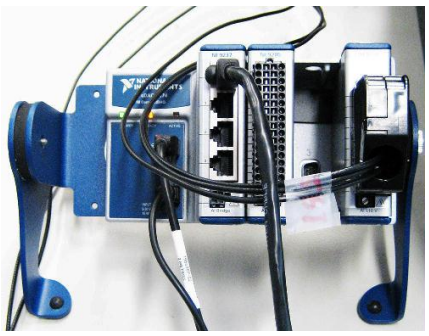

Figure 5 Bridge module for acoustic emission data acquisition.

3. Test Procedure

Under the concentrated load, the loading process of fracture instability of double-layer rock plates were as follows:

Firstly,assemble the spontaneously developed loading device in order.

Secondly, according to combining form, place the sandstone plates on the rotatable bearing of both ends of the loading framework.

Thirdly, regulate four nuts to keep the steel plates of both sides of the loading framework vertical and make the steel plates clamp the double-layer rock plates.

Fourthly, place the loading device equipped with specimens on the loading cushion of the MTS-851 rock mechanics testing machine horizontally.

Fifthly, place the loading circular plate on the rock plates and adjusting the position of the steel ball of the loading plate to the centroid of sandstone plates.

Finally, place the acoustic emission probe on one side of rigid contact with tape and apply the load on the rock plates with MTS-851 rock mechanics testing machine to conduct the test.

4. Test Results and Analysis

4.1. Characteristics of load-displacement curves

Through twelve sets of experiments, it was found that the load-displacement curves had the common features. As shown in Fig. 6, there were generally four distinct mechanical response stages in the load-displacement curves of double-layer rock plates, taking the combination of upper thin plate and lower thick plate as an example.

The first stage: the horizontal initial stage of load-displ-acement curve. This stage mainly included contact adjustment between the loading contactor and sandstone plates, which was initial-load (or initial-displacement) adjustment.

The second stage: when the applied load reached to the firs peak (approximately 2.0 kN), there were smaller vertical displacements in upper thin plate, the fracture developed and then the peak dropped. There was a linear relationship between the load increment and displacement increment and this stage showed the brittle failure feature.

The third stage: with the vertical displacement increasing, the applied load showed an significant growth trend. After reaching the second peak, there was a through-and-through fracture in the upper thin plate and lag fracture in the lower thick plate. Then the load dropped again. This stage showed the brittle failure feature too.

The fourth stage: as the load continued to increase after the second peak (approximately 5.2 kN), there were integral fracture and instability occurred in three sets of specimens and the load dropped at last. The loads varied greatly depending on variation of displacement and the double-layer rock plates of the integral fracture and instability showed plastic deformation feature.

Although three sets of double-layer rock plates had the same mechanical behavior before the second load peak, after that the combined specimens showed three different types of mechanical behavior of the sandstone plates: the first set showed post-peak yielding platform, the second set showed post-peak hardening behavior and the third set showed post-peak softening behavior. Overall, bearing capacity of the double-layer rock plates was greater than that of single-layer rock plates.

The other sandstone plates, such as the upper thick plate and the lower thin plate, double thick plates and double thin plates, had the same features of load-displacement curve as the above.

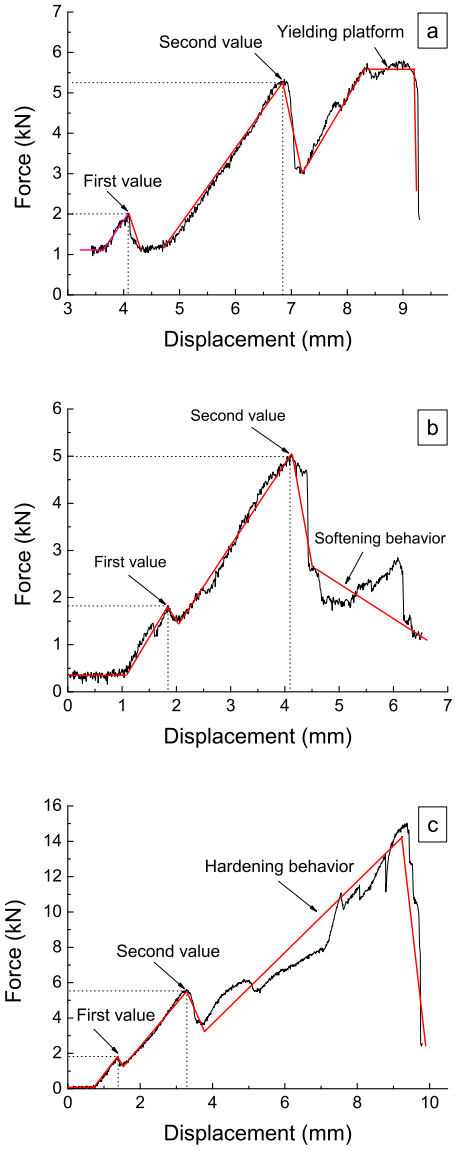

Figure 6 The load-displacement relationship curves. (a) Case 1; (b) Case 2; (c) Case 3

4.2. Characteristics of load-time-acoustic emission event rate curves

AE is a phenomenon of transient elastic-wave generation due to a rapid release of strain energy caused by a structural alteration in a solid material. Acoustic emission event is closely related to the deformation and fracture mechanism.

As shown in Fig. 7, the force-time-acoustic emission event rate curves of double-layer rock plates showed the features as follows:

At horizontal initial stage of the load-displacement curves, when the load was small, there were few or no acoustic emission events (Figs. 7b and 7c). When the load was larger, there were a few acoustic emission events because of machining accuracy and the interaction between the sandstone plates, but the force-time-acoustic emission event rate was low.

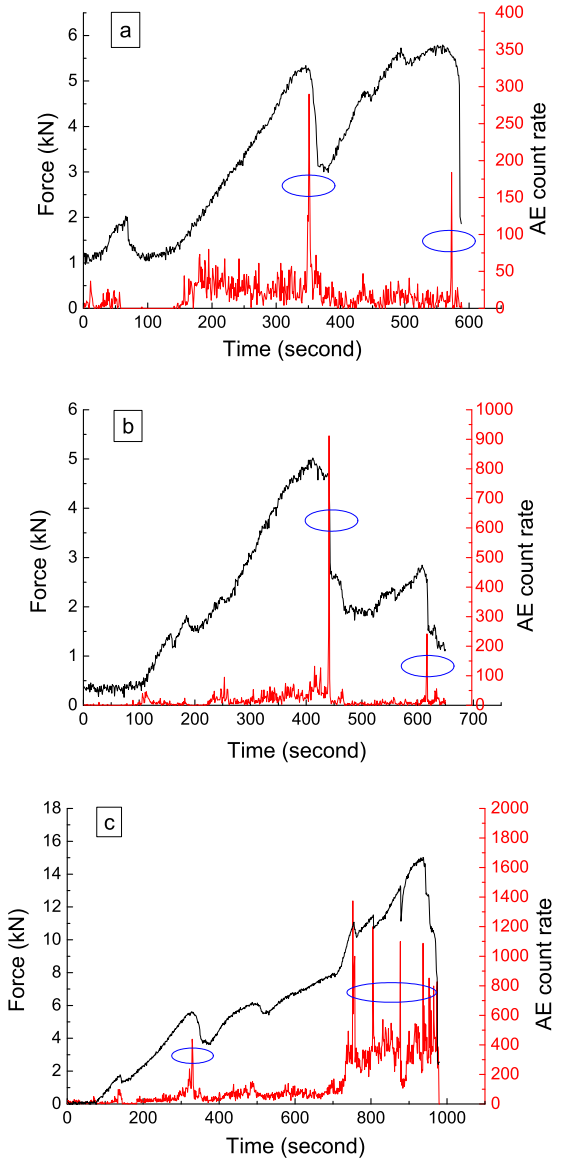

Figure 7 The load-time-acoustic emission event rate curves. (a) Case 1; (b) Case 2; (c) Case 3

When the applied load reached to the second peak and before the integral fracture and instability occurrence, there were more acoustic emission events and higher acoustic emission event rate occurred due to the macro crack propagation and coalescence of rock plates (Figs. 7a and 7c). By contrast, the load varied little with the displacement, micro-cracks in the rock plates increased gradually and the crack propagation and coalescence did not occur in pre-peak phase, so acoustic emission events were kept at a constant level and the acoustic emission event rate was relatively stable. But in the phase between the second peak and the load peak dropping, there were a number of the crack propagations and coalescences occurred because the load varied significantly with the displacement, so there were more acoustic emission events and higher acoustic emission event rate (Fig. 7c), which suggested, the crack propagations and macro coalescences were remarkable.

As shown in Fig. 7b, in the phase between the second peak and the load dropping there were more acoustic emission events and higher acoustic emission event rate because of the crack propagation and coalescence.

It was clear that many reasons, such as uneven mineral components of the rock, the error of machining accuracy and bad connection between the double-layer rock plates, all caused the acoustic emission complicated. The test results indicated that the acoustic emission events were not only in the pre-peak phase, but also in the post-peak phase. Although the AE could not explain accurately, it could be generally an assistant method to monitor the initiation, development, fusion and coalescence of inner micro-crack of the specimens and it was positive to reveal the failure mechanism and the complicated mechanical mechanism of rock plates.The other sandstone plates, such as the upper thick plate and the lower thin plate, double thick plates and double thin plates, had the same features of force-time-acoustic emission event rate curves as the above mentioned.

4.3. Fracture instability and failure models of the combined rock plates

In the test, the cracks propagated from bottom to top along the cross section in the middle of the upper thin plate under the concentrated load. As the load increasing, the coalescence phenomenon occurred finally. The lower plate was cracked later than the upper thin plate, the cracks propagated from bottom to top along the cross section in the middle as the upper thin plate too, and both of them had the same position and direction of crack initiation.

As shown in Fig. 8, the surface crack of the upper thin plate of sandstone plates distributed radially under the concentrated load, and which showed the plate-fracture feature; the lower thick plate showed the beam-fracture feature along the main crack in middle of the thick plate. Due to the end effects of rock plates, there showed three sets of fractures in Fig. 8c.

The experimental study showed that the double-layer rock plates, nearly all the upper plates had the radial plate-fracture feature and nearly all the lower plate had the beam-fracture feature in different plate combinations.

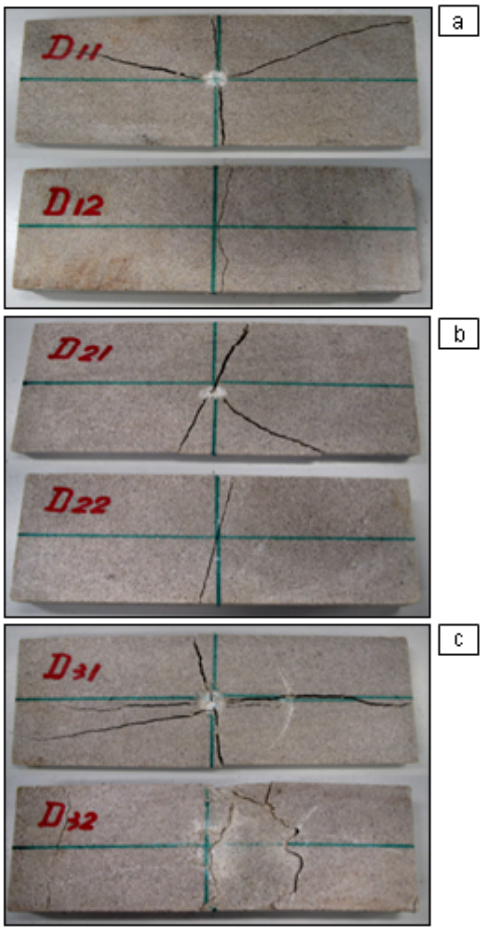

Figure 8 T The surface crack distribution map of the rock plates. (a) Case 1; (b) Case 2; (c) Case 3

Particularly noteworthy was that as shown in Fig. 9, two upper thick plates showed the arch-fracture feature in the two sets of rock plates, which showed as the thickness increased, the chance of having arch-fracture in the upper plate would increase too.

5. Conclusion

The fracture instability process of double-layer rock plates test were conducted by the new loading device, and the device is simple, economic, and operable.

There were four distinct mechanical response stages in the force-displacement curves of double-layer rock plates. The double-layer rock plates had the same mechanical behaviors before the second load peak, and three types of mechanical behavior of the double-layer rock plates arose after the second load peak, which were post-peak yielding, post-peak hardening and post-peak softening.

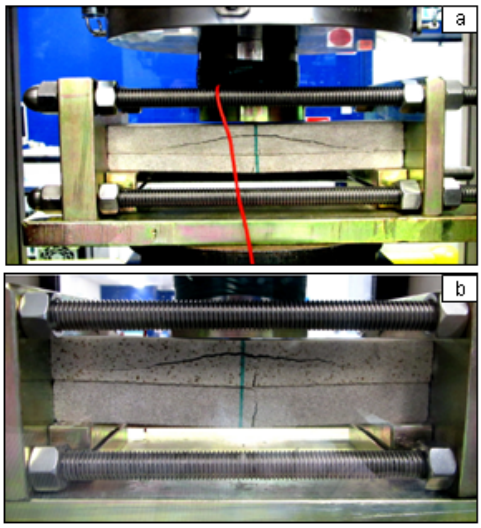

Figure 9 The cross-sectional arched crack distribution map. (a) The upper thick and the lower thin plates; (b) Double layer thick plates

There were many different acoustic emissions among the adjustment phase, the pre-peak phase and the post-peak phase of force-time-acoustic emission event rate curves; it could reveal mechanical mechanism for the crack generating, propagation and coalescence of double-layer rock plates in the process of fracture and instability.

The experimental results showed that there were three failure modes of beam fracture, arch destruction and plate fracture damage. And the results above mentioned were instructive to study on the stability and risk prediction of the roof of the mined-out areas.

The combined plates of more than three layers and that with weak intercalated layer will be further studied in the follow-up tests.

Acknowledgement

This work was financially supported by the National Natural Science Foundation of China (51074140), the China Scholarship Council (CSC) & the Hebei Provincial Office of Education (2010813124), and the School of Mining Engineering, University of New South Wales. In the test, Dr. Hossein Masoumi had made the sandstone samples, Mr. Kanchana Gamage operated the MTS-851 rock mechanics testing machine, Allen Roberts produced the loading devices, Dr. Mojtaba Bahaaddini and Dr. Chengguo Zhang had given us many helps, all these are gratefully acknowledged.

References

[1] Tong L.Y., Liu S.Y., Qiu Y. and L. Fang, Current research state of problems associated with mined-out regions under expressway and future development, Chinese Journal of Rock Mechanics and Engineering, **23**, 1198-1202 (2004).

[2] Zhang X.Y., Analysis of creep damage fracture of upper roof, Journal of Liaoning Technical University (Natural Science Edition), **28**, 777-780 (2009).

[3] Zhang X.Z., Chen H.Q. and Z.Y. Wang, On the acoustic emission characteristics of concrete fracture subjected to three-point-bending, Journal of Experimental Mechanics, **25**, 457-462 (2010).

[4] Swift G.M. and D.J. Reddish, Stability problems associated with an abandoned ironstone mine, Bulletin of Engineering Geology and the Environment, **61**, 227-239 (2002).

[5] Nomikos P.P., Sofianos A.I. and C.E. Tsoutrelis, Structural response of vertically multi-jointed roof rock beams, International Journal of Rock Mechanics & Mining Sciences, **39**, 79-94 (2002).

[6] Diederichs M.S. and P.K. Kaiser, Tensile strength and abutment relaxation as failure control mechanisms in underground excavations, International Journal of Rock Mechanics & Mining Sciences, **36**, 69-96 (1999).

[7] He G.L., Li D.C., Zhai Z.W. and G.Y. Tang, Analysis of instability of coal pillar and stiff roof system, Journal of China Coal Society, **32**, 897-901 (2007).

[8] Wang J.A., Li D.Z. and X.C. Shang, Mechanics analysis on creep fracture of strong roof strata above mined-out area, Journal of University of Science and Technology Beijing, **33**, 142-147 (2011).

[9] Cravero M. and G. Iabichino, Analysis of the flexural failure of an overhanging rock slab, Int. J. Rock Mech. Min. Sci., **41**, 1-6 (2004).

[10] Wang S.R. and H.H. Jia, Analysis of creep characteristics of shallow mined-out areas roof under low stress conditions, Applied Mechanics and Materials, 105-107, 832-836 (2012).

[11] Wang S.R., Jia H.H. and C.F. Wu, Determination method of roof safety thickness in the mined-out regions under dynamic loading and its application, Journal of China Coal Society, **35**, 1263-1268 (2010).

[12] Wu S.X., Zhang S.X., D.J. Shen, An experimental study on Kaiser effect of acoustic emission in concrete under uniaxial tension loading, China Civil Engineering Journal, **41**, 31-39 (2008).

[13] Miao S.J., Lai X.P., Zhao X.G. and F.H. Ren, Simulation experiment of AE-based localization damage and deformation characteristic on covering rock in mined-out area, International Journal of Minerals, Metallurgy and Materials, **16**, 255-260 (2009).

[14] Zhao X.D., Li Y.H., Yuan R.B., Yang T.H. and J.Y. Zhang, Study on crack dynamic propagation process of rock samples based on acoustic emission location, Chinese Journal of Rock Mechanics and Engineering, **26**, 944-950 (2007).

[15] Raposo C.A., Bastos W.D. and J.A.J. Avila, A transmission problem for Euler-Bernoulli beam with Kelvin-Voigt damping, Applied Mathematics and Information Science, **5**, 17-28 (2011).

Shuren Wang is one professor from the School of Civil Engineering and Mechanics, Yanshan University, China. He obtained his Ph.D. degree from University of Science and Technology (Beijing). And he has been worked as a visiting scholar at the School of Mining Engineering, the University of New South Wales, Australia. He is an active researcher in mining engineering, geotechnical engineering, soil mechanics and numerical simulation, and has published more than 50 research articles in journals of the related fields.

Paul Hagan received the Ph.D. degree in Mining Engineering, the University of New South Wales in 1990. He is currently working in the University of NSW, Australia. His research interests are in the areas of machine cutting of rock and rock support systems.

Yan Cheng received the B.S. degree from the Shool of Resources and Safety Engineering, Central South University, China. Now she is a doctor student at School of Mining Engineering, the University of NSW, Australia. Her interested research is mining engineering and acoustic emission technology.